

1 *This is the peer reviewed version of the following article: Martin-Piñero, M.J., García, M.C.,*
2 *Santos, J., Alfaro-Rodríguez, M.-C. and Muñoz, J. (2020), Characterization of novel*
3 *nanoemulsions, with improved properties, based on rosemary essential oil and biopolymers. J Sci*
4 *Food Agric, 100: 3886-3894., which has been published in final form at*
5 *<https://doi.org/10.1002/jsfa.10430> . This article may be used for non-commercial purposes in*
6 *accordance with Wiley Terms and Conditions for Use of Self-Archived Versions. This article may*
7 *not be enhanced, enriched or otherwise transformed into a derivative work, without express*
8 *permission from Wiley or by statutory rights under applicable legislation. Copyright notices must not*
9 *be removed, obscured or modified. The article must be linked to Wiley's version of record on Wiley*
10 *Online Library and any embedding, framing or otherwise making available the article or pages*
11 *thereof by third parties from platforms, services and websites other than Wiley Online Library must*
12 *be prohibited*

13
14
15 **Characterization of novel nanoemulsions, with improved properties, based on**
16 **rosemary essential oil and biopolymers.**

17 M José Martin-Piñero^a, M Carmen García^a, Jenifer Santos^a, Maria-Carmen Alfaro-
18 Rodríguez^{a*} and José Muñoz^a.

19 ^a Departamento de Ingeniería Química, Facultad de Química, Universidad de Sevilla, C/
20 P. García González, 1, E41012, Sevilla, Spain.

21 * Corresponding author: Maria-Carmen Alfaro-Rodríguez; Tel.: +34 954 557180; fax:
22 +34 954 556447; E-mail address: alfaro@us.es

23 **Abstract**

24 **BACKGROUND:** Nowadays, it is of great interest to develop stable and sustainable
25 formulations that act as nanocarriers of active ingredients. In this work, the droplet size
distribution, rheology and physical stability of nanoemulsions with improved properties
containing rosemary essential oil and biopolymers as a function of the concentration of
these polysaccharides was investigated.

RESULTS: Mean diameters below 150 nm were achieved, indicating nanostructures
were obtained. Regardless of gum type, a gel-like structure and a shear thinning behaviour
was achieved. In addition, an increase of G' , G'' and viscosity and a decrease of J_0 , J_1 , J_2 ,
 λ_1 and λ_2 with increasing gum concentration were observed, due to the formation of a
three-dimensional network in the aqueous phase. Slight differences between
nanoemulsions containing welan or xanthan were found. Creaming, depletion
flocculation and gel aggregation were the main destabilization processes at low,
intermediate and high gum concentration, respectively. 0.4 wt% gum nanoemulsion
exhibited the best physical stability.

CONCLUSION: These stable and sustainable nanoemulsions with improved rheological
properties contribute to the development of biodegradable and non-toxic food or

26 agrochemical products.

27

28 **Keywords:** Nanoemulsion, rosemary essential oil, biopolymer, rheology, physical
29 stability.

30

31

32

33

34

35

36

37

38

39

40

41

42

43

44

45

46

47

48

49

50

51

52

53

54

55

56

57

58

59

60

61

62

63

64

65

66 1. INTRODUCTION

67 In recent years, numerous studies about nanoemulsions have been developed due to the
68 interest of these formulations as delivery systems for lipophilic active compounds.
69 However, nanoemulsions are Newtonian and lack the desired rheological properties for
70 some applications. Thus, for example in the case of an emulsion-based agrochemical or
71 food product, this product should possess a non-Newtonian behaviour with high viscosity
72 at rest in order to prevent its destabilization during lifetime, but at the same time, with
73 low viscosity under an applied stress in order to facilitate the handling. In addition, a gel-
74 like structure is also interesting due to the fact that is correlated with a higher stability of
75 emulsions against creaming. This rheological behaviour can be obtained with these
76 structured nanoemulsions which can be used not only in agrochemical or food
77 applications but also in pharmaceutical, medical or cosmetic applications. Currently,
78 another aspect to consider when formulating a product is the growing interest of
79 consumers in the use of natural products and sustainable raw materials.

80 Natural polymers, actually strongly demanded due not only to their thickening, stabilizing
81 or emulsifying properties, but also their biocompatibility, biodegradability and non-
82 toxicity, can be used to enhance the rheological properties and improve the shelf life of
83 nanoemulsions. Specifically, xanthan gum advanced performance and welan gum were
84 used in this study.

85 Xanthan gum (XG) is a natural high molecular weight anionic polysaccharide produced
86 by aerobic fermentation of sugars by the microorganism *Xanthomonas campestris*.¹ There
87 are numerous products in different fields which use xanthan gum. Cleaners, coatings,
88 polishes and products in the agricultural and food industry also use xanthan gum.²
89 Specifically, advanced performance food grade xanthan gum is suitable for sauces, milk
90 and cream products or beverages.

91 Welan gum is an anionic extracellular polysaccharide produced by the micro-organism
92 *Sphingomonas sp.*, namely from *Alcaligenes sp.*, ATCC 31555.³ Although welan gum is
93 rarely used in emulsions, in the last few years, there have been a number of studies
94 concerning its use in this type of formulations. For example, welan gum may be used as
95 an ingredient in food products in which it can act as a thickening, suspending, binding,
96 emulsifying, stabilizing and viscosifying agent.³

97 The high antioxidant and antibacterial activity of REO against *L. monocytogenes*
98 bacteria and also against *Escherichia coli*, *Salmonella indiana* and *Listeria innocua* has
99 been attributed to the presence of its main components such as α - pinene, 1,8-cineole,

100 camphor, myrcene, camphene, borneol and verbenone.⁴⁻⁶ REO is used in a wide range of
101 applications, such as in food, in cosmetics, in nutraceuticals, agrochemical,
102 phytomedicines and aromatherapeutical products.^{7,8}

103 In this study, a non-ionic surfactant known as Appyclean 6548 was used. This surfactant
104 belongs to the alkyl polyglucoside (APG) group. Appyclean is a family of
105 environmentally friendly surfactants possessing an Ecocert certificate, which are very
106 desirable for using in green formulations. Rosemary oil/water emulsions has been
107 demonstrated to have high physical stability using Appyclean 6548 (D-glucose,
108 oligomeric C14/18 alkylglycoside) as surfactant.⁹ However, this system exhibits low
109 viscosity, a Newtonian flow behaviour and lacks a linear viscoelastic region. In addition,
110 this emulsion suffers a destabilization by creaming. It is to be expected that the addition
111 of gum causes the formation of a network capable of delaying the creaming and providing
112 viscoelasticity to the nanoemulsion. Thus, the development of sustainable nanoemulsions
113 with desirable rheological characteristic could be achieved by varying the concentration
114 of gum. Therefore, the main objective of this work was to study the influence of the
115 concentration of two different polysaccharides (welan and xanthan advanced
116 performance gum) on the droplet size distribution, rheology and physical stability of
117 nanoemulsions formulated with REO and Appyclean 6548, a non-ionic and renewable
118 bio-based surfactant. These stable and sustainable nanoemulsions with improved
119 rheological properties can be useful to the food and agrochemical industries as food
120 preservative or insecticide due to the antimicrobial properties of the rosemary oil.^{10,11}
121 Furthermore, they can be useful to develop lipophilic active-loaded products with novel
122 applications.

88

89 2. MATERIALS AND METHODS.

90 *Materials.*

91 All components of nanoemulsions are derived from natural sources. Thus, the surfactant
92 is wheat-derived, while the dispersed phase is rosemary essential oil (REO) which is
93 distilled from *Rosemarinus officianalis* L. REO was supplied by Sigma Aldrich (Spain)
94 and Appyclean 6548 was purchased from Wheatoleo (France). Additionally, xanthan gum
95 (KELTROL® Advanced Performance) of molecular weight about $2 \cdot 10^6$ /mol and welan
96 gum (K1A96) of molecular weight about $6.6 \cdot 10^5$ g/mol were used as stabilizing

97 biopolymers. Both gums were kindly provided by CP Kelco Company (San Diego, USA).
98 Ultrapure water was used to prepare the aqueous phase.

99 *Emulsification Procedure.*

100 The aqueous phases were prepared by dissolving 0.1/100 g sodium azide in ultrapure
101 water cleansed using a Milli-Q water purification system. The dispersed phases were
102 formed by the emulsifier, Appyclean 6548 (4/100 g), and rosemary oil (20/100 g).
103 Emulsions were prepared following the protocol reported by Martin-Piñero.⁹ Finally, in
104 order to obtain the structured nanoemulsion, the gum was added very slowly into the final
105 emulsions at room temperature. The emulsions were mechanically stirred using an Ultra-
106 turrax device (IKA Janke and kunkel, IKA-Labortechnik) for two hours up to a maximum
107 of 520 x g (800rpm). A total of 11 samples were prepared using different kinds of
108 biopolymer (xanthan and welan gums) at different concentrations (0, 0.1/100, 0.2/100,
109 0.3/100, 0.4/100, 0.5/100 g).

110 *Droplet size distribution (DSD) measurements.*

111 Size distribution of oil droplets was determined by the laser diffraction technique
112 (Mastersizer 2000, Malvern, Worcestershire, United Kingdom). Aging time evolution of
113 the volume-weighted mean diameter ($D_{4,3}$) of the emulsion droplets and the span values
114 were studied for 28 days. $D_{4,3}$ values were obtained from the following equation:

115115
$$D_{4,3} = \frac{\sum_{i=1}^N n_i d_i^4}{\sum_{i=1}^N n_i d_i^3} \quad (\text{Eq. 1})$$

116 where n_i is the number of droplets with diameter d_i . On the other hand, span values are
117 given by:

118118
$$\text{Span} = \frac{D(v,0.9) - D(v,0.1)}{D(v,0.5)} \quad (\text{Eq. 2})$$

119 where $D(v, 0.9)$, $D(v, 0.5)$ and $D(v, 0.1)$ are the highest droplet size contained in 90%,
120 50% and 10% of volume of dispersed phase, respectively.

121 *Physical Stability.*

122 The physical stability of rosemary essential oil nanoemulsions was evaluated for 28 days
123 at 30°C by a Turbiscan Lab Expert device (Formulation, Toulouse, France) using the
124 multiple light scattering technique. Emulsion stability was studied by analysing the
125 variation of the backscattering (BS) profiles as a function of time. The intensity of the

126 scattered light makes it possible to determine the major mechanism of destabilization in
127 each sample as well as the kinetics of the destabilization process.

128 *Rheology.*

129 Flow curves were performed with a Modular Advanced Rheometer System (Haake
130 MARS, Thermo Electron Corp., Germany) and a double cone geometry (60/1°) for
131 nanoemulsions with gum concentration lower than 0.3/100 g. Nanoemulsions with
132 0.4/100 g and 0.5/100 g of gums were measured using a serrated plate-plate sensor (60
133 mm). Flow curves were carried out in a range of 0.05 to 20 Pa.

134 Frequency sweeps were obtained from 0.05 to 15 rad/s at fixed shear stress within the
135 linear viscoelastic region. Creep experiments were performed for constant shear stresses
136 (0.05 Pa) for 3600 s.

137 Equilibration time prior to rheological tests was 300s. All measurements were performed
138 at $20\text{ °C} \pm 0.1\text{ °C}$ using a C5P Phoenix circulator (Thermo-Scientific, Germany).

139 All measurements were carried out in triplicate and the values shown are the average of
140 the three replicates. The standard deviation of all measurements was lower than 5-10%
141 for all the samples.

142 *Statistical analysis.*

143 A general linear model – one-way ANOVA – was used to determine significant
144 differences ($P \leq 0.05$) between samples, followed by the post-hoc Tukey HSD test. All
145 statistical treatments were done with the software Infostat, version 2017 (Facultad de
146 Ciencias Agropecuarias, Universidad Nacional de Cordoba, Cordoba, Argentina).

147

148 **3. RESULTS AND DISCUSSION.**

149 **3.1. Droplet Size Distribution**

150 Figure 1 shows as inset, by way of example, the droplet size distribution of the emulsions
151 containing 0.4/100 g WG and 0wt% gum as reference, both 24 hours after preparation.
152 As can be observed, 0wt% gum emulsion is monomodal ($\text{span} = 0.74 \pm 0.01$) and the
153 volumetric weight diameter is 149 ± 6 nm. By contrast, the addition of 0.4/100 g of
154 biopolymer provokes a shift of DSD towards bigger droplets and the distribution was
155 bimodal. In order to gain a deep insight into the results obtained, measurements of laser

156 diffraction at different conditions of dispersion (introducing ultrasounds) as a function of
157 time in the measuring cell were carried out. Results obtained are shown in Figure 1. As
158 can be observed, the droplet size distribution shifted towards smaller droplet sizes and
159 was monomodal. These facts revealed that the emulsion was initially flocculated and
160 proved that the second peak corresponded to air bubbles, which were removed. Therefore,
161 ultrasonics break-up the agglomerates, making it possible to obtain the droplet size of the
162 primary droplets. It should be noted that the addition of gum did not significantly change
163 the DSD compared to the emulsion without gum. However, these results demonstrate the
164 ability of both xanthan gum and welan gum to promote flocculation.

165 Figure 1

166 The influence of gum concentration and ageing time (1 and 28 days) on the values of $D_{4,3}$
167 and span of nanoemulsions are shown in Table 1. These parameters were selected because
168 they were very sensitive to the aggregation of droplets and, therefore, to detect
169 destabilization by coalescence or Ostwald ripening. As can be observed, nanoemulsions
170 containing welan gum exhibited similar volumetric mean diameter 24 hours after
171 preparation, except for the one formulated with 0.4/100 g, which presented the highest
172 values of both $D_{4,3}$ and span. Similar results were found for nanoemulsions containing
173 xanthan gum but it was the nanoemulsion with 0.5/100 g of gum which exhibited the
174 highest values of both parameters. Ageing time has an influence on distribution
175 parameters for nanoemulsions containing 0.3/100 g and 0.5/100 g of WG and for
176 nanoemulsions with 0.3/100 g of APXG. For these nanoemulsions, an increase in
177 volumetric mean diameter and span occurred with time, suggesting the occurrence of a
178 destabilization process by coalescence.^{12,13} It is noteworthy that the increase in droplet
179 size observed is not caused by flocculation due to the fact that the aggregates were broken
180 up before the measurement was carried out, as mentioned above.

181181

182 **3.2. SAOS tests**

183 Regardless of type of gum used, all nanoemulsions exhibited a measurable linear
184 viscoelastic range except the one with 0.1/100 g of biopolymer. For this reason, results at
185 this concentration of gum are not shown. The effects of gum concentration on storage,
186 G' , and loss, G'' , moduli as a function of frequency for microfluidized rosemary O/W
187 emulsions, aged for 24 hours, are shown in Figure 2. All nanoemulsions showed that G'

188 was larger than G'' over the whole measured frequency range, indicating that the elastic
189 component was predominant in the viscoelasticity. Furthermore, a slight frequency
190 dependence of both moduli was found. These profiles are consistent with a weak gel-like
191 viscoelastic structure and they indicate more semi-solid-like than liquid-like behaviour.
192 As expected, G' and G'' increased with gum concentration, consistent with a tri-
193 dimensional macromolecular network with more elastic and viscous behaviour. As occurs
194 in gum solutions with gel-like structure, both moduli have an exponential relationship
195 with the gum concentration which was fitted to the following equations:

196
$$\log G' = \log a + b * \log C \text{ (Eq. 3)}$$

197
$$\log G'' = \log a' + b' * \log C \text{ (Eq. 4)}$$

198

199 where b and b' are the power law index of G' and G'' , respectively, and a and a' are elastic
200 coefficient and viscous coefficient, respectively. As can be observed in Table 2, a and a'
201 values were higher for nanoemulsions containing welan gum, indicating that these
202 nanoemulsions are more elastic and viscous than nanoemulsions containing xanthan gum.
203 Likewise, nanoemulsions with welan gum were more dependent on the concentration, as
204 can be deduced from the higher values of the b and b' parameters.

205

Figure 2

206

Table 2

207 From the frequency sweeps, values for loss tangent were calculated. $\tan \delta$ is defined as
208 the ratio of loss modulus and storage modulus, which is used to detect differences in the
209 temporary structure of samples.

210210
$$\tan \delta = \frac{G''}{G'} \text{ (Eq. 5)}$$

211 When the loss tangent approaches zero, the elastic structure of the system predominates,
212 whereas if it exceeds 1 value the system is considered viscous. As shown in Figure 3A,
213 the elastic component predominates over the viscous one over the whole frequency range
214 with $0.23 < \tan \delta < 0.33$ and $0.29 < \tan \delta < 0.68$ for nanoemulsions with APXG and WG,
215 respectively. The $\tan \delta$ values were lower than 1, indicating that the molecular network
216 was strong and permanent.¹⁴ In all cases, $0.1 < \tan \delta < 1$ indicating that these
217 nanoemulsions do not behave as true gels, but as weak gels such as discussed above.

218218

219 All nanoemulsions containing gum as thickener showed a clear minimum in $\tan \delta$ value
220 except for the emulsion with 0.2/100 g WG. From this minimum it is possible to calculate
221 the plateau modulus, G_N^0 :¹⁵

222222
$$G_N^0 = [G']_{\tan \delta \rightarrow \min} \quad (\text{Eq. 6})$$

223223

224 The higher the G_N^0 value, the higher the entanglement density between polymeric
225 molecules.¹⁶ As expected (Figure 3B), an increase in gum concentration caused an
226 increase in the plateau modulus value, indicating an increase in the entanglement density.
227 It should be noted that the values of plateau modulus are slightly higher in nanoemulsions
228 containing welan gum than those containing xanthan gum.

229 All results are consistent with a double helix conformation for both gums. However, it
230 seems strange that welan gum, despite having lower molecular weight than xanthan,
231 provides nanoemulsions with greater viscoelasticity. This result could be explained by
232 the fact that welan gum adopts a different distribution pattern.¹⁷

233

Figure 3

234 The evolution with ageing time of G' values at an intermediate frequency within the
235 frequency range studied (6.8 rad/s) for all nanoemulsions is illustrated in Figure 4. Fig. 4
236 shows that for the first days nanoemulsions exhibited a slight tendency to a decrease in
237 G' , made more marked by increasing the concentration of gum in the emulsion.
238 Subsequently, the values remained constant. A decrease in G' with ageing time could be
239 attributed to an increase in droplet size, either by coalescence or by flocculation, which
240 provokes a decrease in the area of contact between droplets, weakening the interactions
241 between them and, therefore, a decrease in elastic properties. All nanoemulsions exhibited
242 values of G' above G'' after 27 days, indicating that the elastic behaviour was preserved.
243 In addition, the nanoemulsions containing welan gum, similarly that happens at 24 h,
244 exhibited higher G' values than those ones formulated with xanthan gum. Note that the
245 results at ageing time higher than 14 days for 0.2/100 g welan gum are not shown due to
246 the breakdown of the emulsion.

247

Figure 4

248 3.3.Creep tests

249 Figure 5 shows creep test results in terms of shear creep compliance versus test time at
 250 constant shear stress (0.05 Pa) as a function of WG and APXG concentration added into
 251 the emulsions. All samples showed a typical response of weak viscoelastic solids with a
 252 non-linear response to strain. As expected, the strongest nanoemulsion, which was the
 253 lowest line, represented the nanoemulsion with 0.5/100 g of concentration of gum added.
 254 The strength of the other samples can be deduced from the level of compliance exhibited
 255 in Figure 5, namely nanoemulsions with 0.4/100 g gum > 0.3/100 g gum.

256 In order to achieve a better analysis of the results, the creep curves were fitted to the
 257 Burger model, which consists of Maxwell and Kelvin elements connected in series. In
 258 this particular case, two elements were used.

$$259259 \quad J(t) = J_0 + \sum_{i=1}^2 J_i (1 - e^{-\frac{t}{\tau_i}}) + \frac{t}{\eta_N} \quad \text{Eq. (7)}$$

260 where J is the compliance as a function of time, t, $J_0 = 1/G_0$ (1/Pa) is the initial
 261 instantaneous compliance, $J_1 = 1/G_1$ and $J_2 = 1/G_2$ are retarded compliances for the Kelvin
 262 model (1/Pa), τ_1 and τ_2 are the retardation time, which is the time needed to reach
 263 maximum deformation for the Kelvin model (s), t is time (s) and η_N is the Newtonian
 264 viscosity (Pa·s) in the steady state.

265 Figure 5

266 All parameters derived from the model are listed in Table 3. The nanoemulsions with
 267 0.5/100 g of gum, regardless of the type of gum, showed the lowest values of J_0 , J_1 , J_2 , λ_1
 268 and λ_2 but the highest value of η_0 . In contrast, the highest values of J_0 , J_1 , J_2 , λ_1 and λ_2
 269 but the lowest value of η_0 was exhibited by the nanoemulsion containing the lowest gum
 270 concentration. These results mean that the structure of nanoemulsions increases their
 271 viscoelastic properties by increasing their gum content due to the fact that they increase
 272 their strength to flow, being more difficult to deform under the imposed stress. From an
 273 overall point of view, no significant differences were observed between the creep
 274 response of nanoemulsions with WG or with APXG.

275 Table 3

276 3.4. Steady state flow tests

277 The flow behaviour of nanoemulsions studied is illustrated, by way of example, for
 278 nanoemulsions containing APXG as a function of their concentration, in Figure 7. It is

279 important to note that emulsion without gum exhibited Newtonian flow behaviour. This
280 Newtonian behaviour has been previously reported by Martín-Piñero et al. (μ
281 $=3.19 \pm 0.02 \text{ mPas}$).⁹ As shown in Figure 6, the addition of gum changes the flow
282 behaviour. Thus, all nanoemulsions presented a shear-thinning behaviour characterized
283 by a decrease in viscosity as the shear rate increased, which is related to the orientation
284 of macromolecules and droplets in the direction of flow. Furthermore, at low shear rates
285 a Newtonian plateau can also be observed up to a critical shear rate. This region is better
286 observed at higher gum concentrations (0.3, 0.4 and 0.5/100 g). The viscosity of this
287 region is so-called zero-shear viscosity (η_0), which is related to the stability of
288 nanoemulsions against creaming.¹⁸ In addition, McClements also indicated that at low
289 shear rates the hydrodynamic forces are not strong enough to break up the flocs, which
290 then act like particles with fixed size and shape, resulting in a constant viscosity. The
291 apparent viscosity of nanoemulsions increased with increasing gum concentration.
292 Obviously, the entanglements of chains of the macromolecules increased with increasing
293 the concentration, which caused the corresponding increase in viscosity.

294 Different models can be used to model the flow behaviour of Non-Newtonian systems,
295 such as Herschel-Bulkley, power law, etc. Nevertheless, for shear thinning fluids, the
296 Cross model is appropriate since it is able to describe this behaviour quite well and in a
297 wide range of shear rates.

298298

$$\eta = \frac{\eta_0}{1 + \left(\frac{\dot{\gamma}}{\dot{\gamma}_c}\right)^{1-n}} \quad (\text{Eq. 8})$$

299 where $\dot{\gamma}_c$ is related to the critical shear rate for the onset of the shear-thinning response,
300 η_0 stands for the zero-shear viscosity and $(1-n)$ is a parameter related to the slope of the
301 power-law region; n being the so-called “flow index”. For shear thinning materials, $0 <$
302 $n < 1$. All nanoemulsions exhibited a good fit to the Cross equation ($R^2 = 0.999$).

303 Zero-shear viscosity values (η_0) and the flow index (n) at 1 and 28 days are shown in
304 Table 4 as a function of the gum type and concentration. Nanoemulsions with welan gum
305 aged for 24 hours exhibited a tendency to a decrease in the critical shear rate with
306 increasing concentration of gum. On the other hand, nanoemulsions with xanthan only
307 show this decrease when increasing the concentration from 0.1 to 0.3/100 g. From this
308 value, it is constant. Except for 0.1/100 g of gum, all nanoemulsions showed a Newtonian
309 region lower than 0.01 s^{-1} , indicating that the emulsion keeps its shear thinning behaviour

310 at low shear rates. The aging time causes an increase in the critical values of the shear
311 rate for the beginning of the shear thinning behaviour.

312 Regarding zero-shear viscosity, at 24 hours of storage time, nanoemulsions with the
313 lowest gum concentration (0.1/100 g) showed the lowest zero-shear viscosity. In contrast,
314 those nanoemulsions containing the highest gum content exhibited the highest viscosity
315 value. In general, by increasing the concentration of gum, an increase in viscosity
316 occurred, irrespective of the nature of the gum. This result may be explained by the
317 thickener effect of biopolymers in the bulk phase.¹⁹

318 At low gum concentration, nanoemulsions with xanthan gum are more viscous than those
319 ones containing welan gum. However, at the highest concentration studied the opposite
320 occurred. Furthermore, nanoemulsions with welan gum turned out to be more dependent
321 on the concentration than those containing xanthan gum, although not significantly. It is
322 noteworthy that the addition of gums into the emulsions to obtain the nanoemulsions not
323 only changes the flow behaviour, but it also considerably increases their viscosity. This
324 augmentation is very significant at the highest gum concentrations (for example, 3.9
325 mPa·s compared to 3000 Pa·s).

326 Except for emulsion with 0.2/100 g of welan gum, zero-shear viscosity decreased for all
327 nanoemulsions after 28 days of study. A decrease in η_0 with aging time could be related
328 to a destabilization of the system by coalescence or flocculation.

329 On the other hand, the low values of the flow index indicated that these nanoemulsions
330 exhibited a strong shear thinning behaviour. The nanoemulsions with lower gum
331 concentration were less shear thinning. In contrast, the nanoemulsions with stronger shear
332 thinning properties were those containing the highest gum concentration. It should be
333 noted that nanoemulsions formulated with xanthan gum are slightly more pseudoplastic
334 than nanoemulsions containing welan gum. The flow indexes slightly increase with
335 ageing time but not significantly.

336 In summary, as expected, η_0 increases and n decreases as a function of gum concentration.
337 On the other hand, ageing time provokes a decrease in viscosity and a decrease in non-
338 Newtonian behaviour.

339 Figure 6

340 Table 4

341 3.5. Multiple light scattering results

342 Profiles of backscattering as a function of the height of the measuring cell and as a
343 function of ageing time for nanoemulsions formulated with xanthan or welan gum at
344 different concentrations of gum are illustrated in Figure 7.

345 Figure 7

346 Different destabilization processes have been found as a function of gum concentration
347 in nanoemulsions. Creaming was the main destabilization process for nanoemulsions with
348 the lowest amount of gum (0.1/100 g for APXG and 0.1/100 g and 0.2/100 g for welan
349 gum). The density difference between continuous and disperse phases besides the low
350 viscosity of these systems favoured gravitational separation. Finally, a layer of serum and
351 a layer of cream were observed. At intermediate gum concentrations (0.2/100 g and
352 0.3/100 g for APXG and 0.3/100 g for welan gum) an increase of droplet size was
353 observed, which can be attributed to a depletion flocculation mechanism caused by the
354 non-adsorbed polymer. This process, sometimes, led to coalescence due to the flocs rise
355 and collide, breaking their interfaces. Depletion flocculation process happened at a higher
356 concentration of gum when welan was used due to its lower molecular weight.²⁰ At a
357 higher gum level (0.4/100 g), nanoemulsions stable against creaming and flocculation
358 were obtained due to the formation of three-dimensional viscoelastic network able to
359 immobilize the droplets. Finally, at the highest gum concentration studied (0.5/100 g) an
360 increase in droplet size (an increase in BS profile over the entire tube length) was
361 observed which was slight for nanoemulsions containing APXG but significant for ones
362 containing welan gum. For latter a destabilization by coalescence occurred according to
363 the results obtained by laser diffraction. We can hypothesize that this concentration of
364 gum is high enough for gel-like aggregates to form, which facilitate the flocculation of
365 droplets and a further coalescence. All results obtained by multiple light scattering were
366 consistent with those obtained by laser diffraction and rheology.

367 Since the destabilization mechanisms of these nanoemulsions are creaming and an
368 increase in the size of droplets (flocculation or/and coalescence), the turbiscan stability
369 index (TSI) was calculated from equation 10 as a global destabilization parameter. This
370 parameter was previously used by other authors:²¹

371371
$$\text{TSI} = \sum \frac{\sum_h |\text{scan}_i(h) - \text{scan}_{i-1}(h)|}{H} \quad (\text{Eq. 9})$$

372 where: $\text{scan}_i(h)$ is the average backscattering for each time (i) of measurement, $\text{scan}_{i-1}(h)$ is the average backscattering for the $i - 1$ time of measurement and H is the number
373 of scans for each sample. Thus, a high value of TSI corresponds to a less stable system.
374 The TSI global values for all nanoemulsions studied are shown in Figure 8. It can be
375 observed that TSI was lower (higher stability) for those samples formulated with 0.4wt%
376 of gum, regardless of the gum type. These two nanoemulsions showed TSI values after
377 28 days of store time of 3.80 and 3.85 for APXG and WG, respectively. Nanoemulsions
378 formulated with lower gum concentration showed the highest values of TSI and a very
379 marked slope at short ageing time, indicating not only their lower stability but also their
380 fast destabilization. Nanoemulsions with 0.5wt% of APXG showed a similar behaviour
381 to 0.4wt%.
382

383 Figure 8

384 **Conclusions.**

385 In this paper, nanoemulsions of rosemary essential oil and biopolymers (advanced
386 performance xanthan or welan gum) were obtained. Firstly, emulsions with rosemary
387 essential oil and a wheat-waste derived surfactant were obtained by microfluidization. In
388 a further step, welan or advanced performance xanthan gum were added. The influence
389 of the gum concentration on the droplet size distribution, rheological properties and
390 physical stability of emulsions was investigated. A gel-like structure and a shear thinning
391 flow behaviour were found. An increase in the gum concentration provoked an
392 augmentation of both the viscoelastic moduli and viscosity and a decrease in J_0 , J_1 , J_2 , λ_1
393 and λ_2 due to the formation of a three-dimensional network in the aqueous phase due to
394 the presence of biopolymers. Emulsions containing welan gum were more elastic and
395 viscous than those containing APXG but, at the same time, they were more dependent on
396 the concentration. Regarding the droplet sizes, nanoemulsions were obtained. $D_{4,3}$
397 remained stable over time except for nanoemulsions containing 0.3/100 g of xanthan gum
398 and those formulated with 0.3/100 g and 0.5/100 g of welan gum, which exhibited
399 coalescence. Different destabilization mechanisms were found, depending on the gum
400 concentration. Creaming was the main destabilization process at low gum level and
401 depletion flocculation, sometimes with coalescence, at intermediate gum level. At 0.4/100
402 g of gum, stable nanoemulsions were obtained and, finally, at 0.5/100 g of gum a new
403 trend to destabilization was observed, which was significant for nanoemulsions

404 containing welan gum, probably due to the formation of gel-like aggregates. Slight
405 differences were observed between nanoemulsions with xanthan or welan which could be
406 explained by the differences in viscosity and molecular weight of both polysaccharides.
407 This work contributes to attempts to meet the demand from consumers for more
408 biodegradable, biocompatible and non-toxic food or agrochemical products..

409409

410 **Acknowledgements**

411 The financial support received (Project CTQ2015-70700-P) from the Spanish Ministerio
412 de Economía y Competitividad and from the European Commission (FEDER
413 Programme) is kindly acknowledged.

414414

415 **Conflicts of interest**

416 The authors declare no conflict of interest.

417 **References**

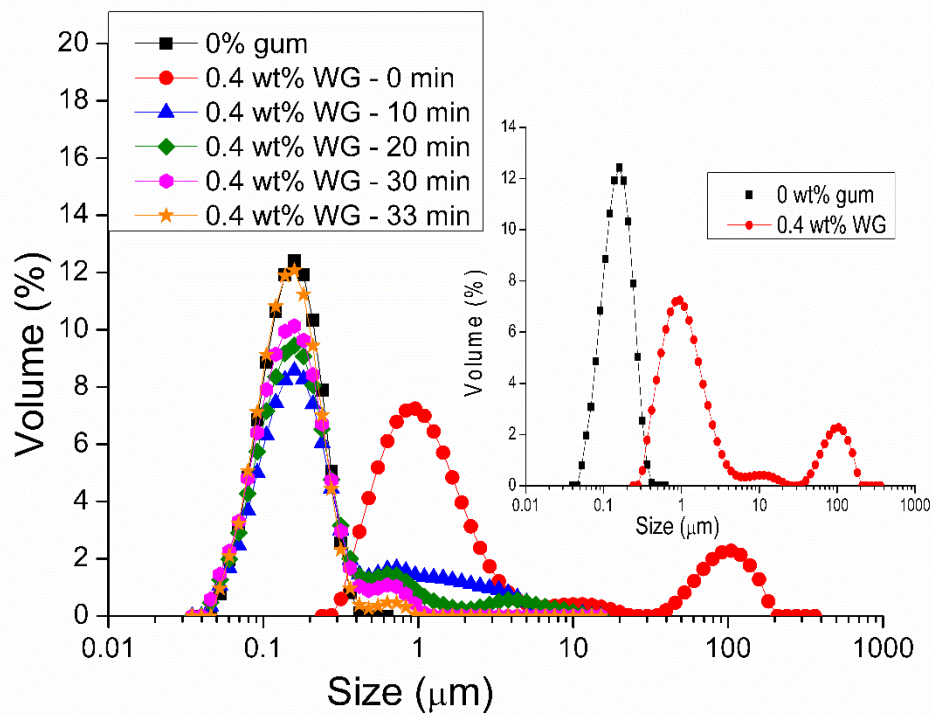
- 418 1 Krstonošić V, Dokić L, Nikolić I, and Milanović M. Influence of xanthan gum on
419 oil-in-water emulsion characteristics stabilized by OSA starch. *Food Hydrocoll*
420 **45**:9–17 (2015).
- 421 2 Katzbauer B. Properties and applications of xanthan gum. *Polym Degrad Stab*
422 **59**:81–84 (1998).
- 423 3 Kaur V, Bera MB, Panesar PS, Kumar H, and Kennedy JF. Welan gum:
424 Microbial production, characterization, and applications. *Int J Biol Macromol*
425 **65**:454–461 (2014).
- 426 4 Abdullah BH, Hatem SF, and Jumaa W. A Comparative Study of the
427 Antibacterial Activity of Clove and Rosemary Essential Oils on Multidrug
428 Resistant Bacteria. *UK J Pharm Biosci* **3**:18 (2015).
- 429 5 Mathlouthi N, Bouzaienne T, Oueslati I, Recoquillay F, Hamdi M, Urdaci M, and
430 Bergaoui R. Use of rosemary, oregano, and a commercial blend of essential oils
431 in broiler chickens: In vitro antimicrobial activities and effects on growth
432 performance1. *J Anim Sci* **90**:813–823 (2012).
- 433 6 Mezza GN, Borgarello A V., Grosso NR, Fernandez H, Pramparo MC, and
434 Gayol MF. Antioxidant activity of rosemary essential oil fractions obtained by

- 435 molecular distillation and their effect on oxidative stability of sunflower oil.
436 *Food Chem* **242**:9–15 (2018).
- 437 7 Borges RS, Lima ES, Keita H, Ferreira IM, Fernandes CP, Cruz RAS, Duarte JL,
438 Velázquez-Moyado J, Ortiz BLS, Castro AN, Ferreira JV, Silva Hage-Melim LI
439 da, and Carvalho JCT. Anti-inflammatory and antialgic actions of a
440 nanoemulsion of *Rosmarinus officinalis* L. essential oil and a molecular docking
441 study of its major chemical constituents. *Inflammopharmacology* **26**:183–195
442 (2018).
- 443 8 Villareal MO, Ikeya A, Sasaki K, Arfa A Ben, Neffati M, and Isoda H. Anti-
444 stress and neuronal cell differentiation induction effects of *Rosmarinus officinalis*
445 L. essential oil. *BMC Complement Altern Med BMC Complementary and*
446 *Alternative Medicine*; **17**:549 (2017).
- 447 9 Martín-Piñero MJ, Ramírez P, Muñoz J, and Alfaro MC. Development of
448 rosemary essential oil nanoemulsions using a wheat biomass-derived surfactant.
449 *Colloids Surfaces B Biointerfaces* **173**:486–492 (2019).
- 450 10 García-Sotelo D, Silva-Espinoza B, Pérez-Tello M, Olivás I, Álvarez-Parrilla E,
451 González-Aguilar GA, and Ayala-Zavala JF. Antimicrobial activity and thermal
452 stability of rosemary essential oil:β-cyclodextrin capsules applied in tomato
453 juice. *LWT* **111**:837–845 (2019).
- 454 11 Hassanzadazar H, Yousefizadeh S, Ghafari A, Fathollahi M, and Aminzare M.
455 Antimicrobial Effects of the Nanoemulsion of Rosemary Essential Oil against
456 Important Foodborne Pathogens. *J Human, Environ Heal Promot* **5**:79–85
457 (2019).
- 458 12 Santos J, Calero N, Trujillo-Cayado LA, García MC, and Muñoz J. Assessing
459 differences between Ostwald ripening and coalescence by rheology, laser
460 diffraction and multiple light scattering. *Colloids Surfaces B Biointerfaces*
461 **159**:405–411 (2017).
- 462 13 Martín MJ, Trujillo LA, García MC, Alfaro MC, and Muñoz J. Effect of
463 emulsifier HLB and stabilizer addition on the physical stability of thyme essential
464 oil emulsions. *J Dispers Sci Technol* **39**:1627–1634 (2018).
- 465 14 Tunick MH. Small-Strain Dynamic Rheology of Food Protein Networks. *J Agric*

- 466 *Food Chem* **59**:1481–1486 (2011).
- 467 15 Wu S. Chain structure and entanglement. *J Polym Sci Part B Polym Phys*
468 **27**:723–741 (1989).
- 469 16 Ferry JD. Viscoelastic properties of polymers. *Viscoelastic Prop. Polym.* 1980.
- 470 17 Xu L, Xu G, Liu T, Chen Y, and Gong H. The comparison of rheological
471 properties of aqueous welan gum and xanthan gum solutions. *Carbohydr Polym*
472 **92**:516–522 (2013).
- 473 18 McClements DJ. Critical review of techniques and methodologies for
474 characterization of emulsion stability. *Crit Rev Food Sci Nutr* **47**:611–649
475 (2007).
- 476 19 Martin-Piñero MJ, García MC, Muñoz J, and Alfaro-Rodríguez MC. Influence of
477 the welan gum biopolymer concentration on the rheological properties, droplet
478 size distribution and physical stability of thyme oil/W emulsions. *Int J Biol*
479 *Macromol* **133**:270–277 (2019).
- 480 20 Grundy MML, McClements DJ, Ballance S, and Wilde PJ. Influence of oat
481 components on lipid digestion using an in vitro model: Impact of viscosity and
482 depletion flocculation mechanism. *Food Hydrocoll* **83**:253–264 (2018).
- 483 21 Trujillo-Cayado LA, Alfaro MC, Santos J, Calero N, and Muñoz J. Influence of
484 primary homogenization step on microfluidized emulsions formulated with
485 thyme oil and Appyclean 6548. *J Ind Eng Chem* **66**:203–208 (2018).

486486

487 Figures

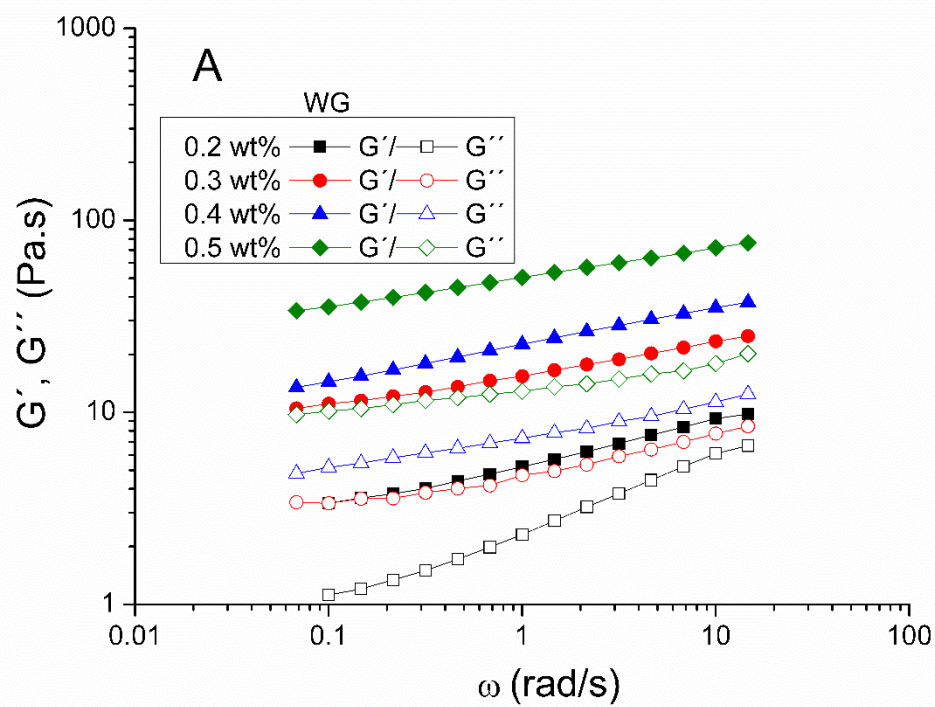


488488

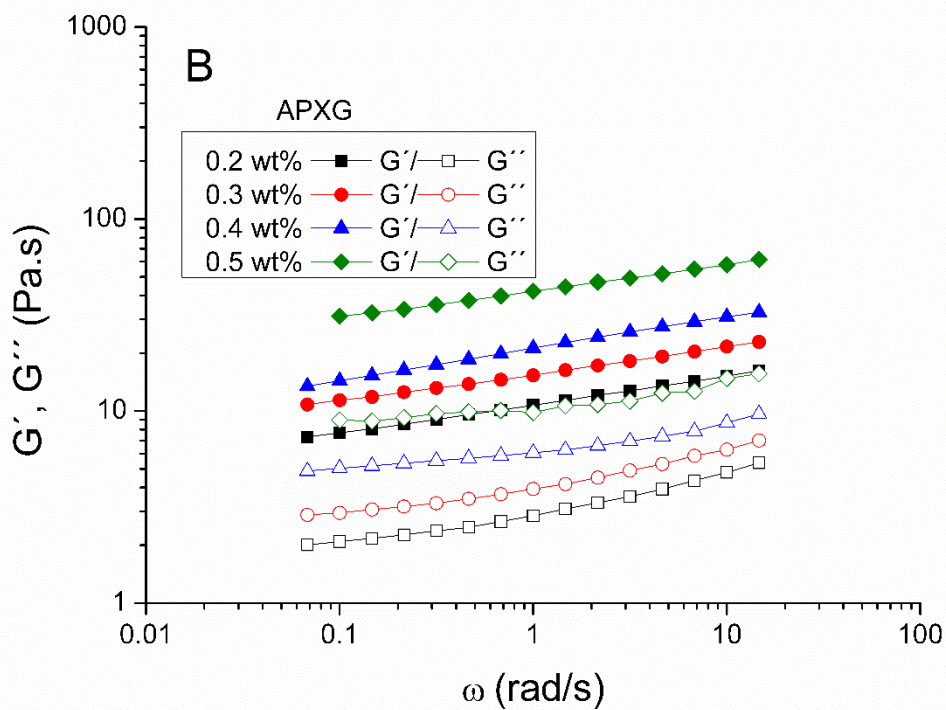
489 Figure 1. Droplet size distribution for emulsions containing 0.4wt% of WG as function of
 490 ultrasound time in the measurement cell and as inset, 0.4 wt% WG without ultrasound and 0
 491 wt% gum

492

493

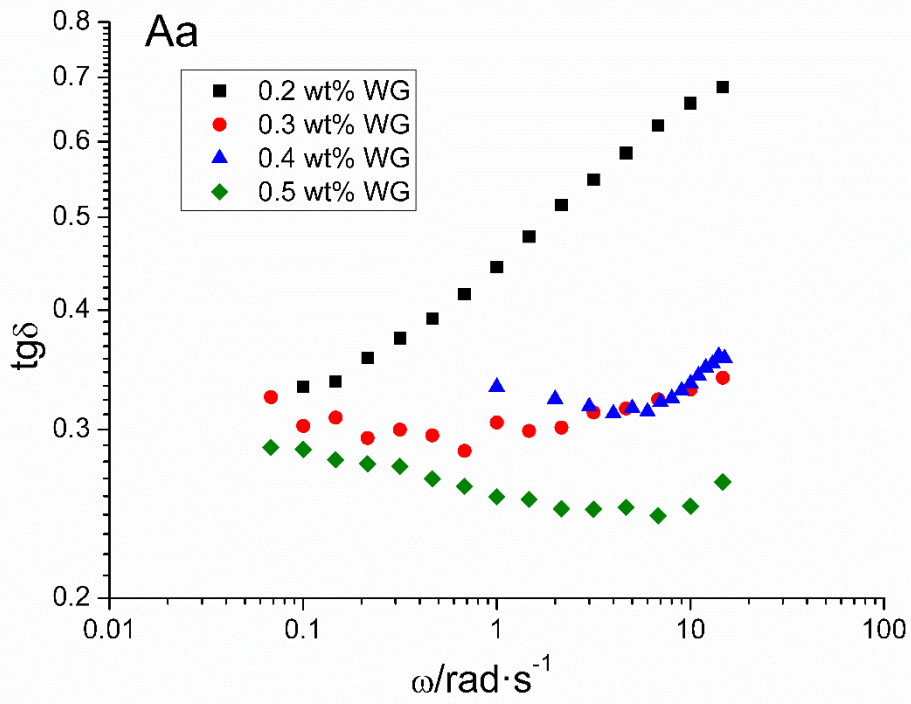


494

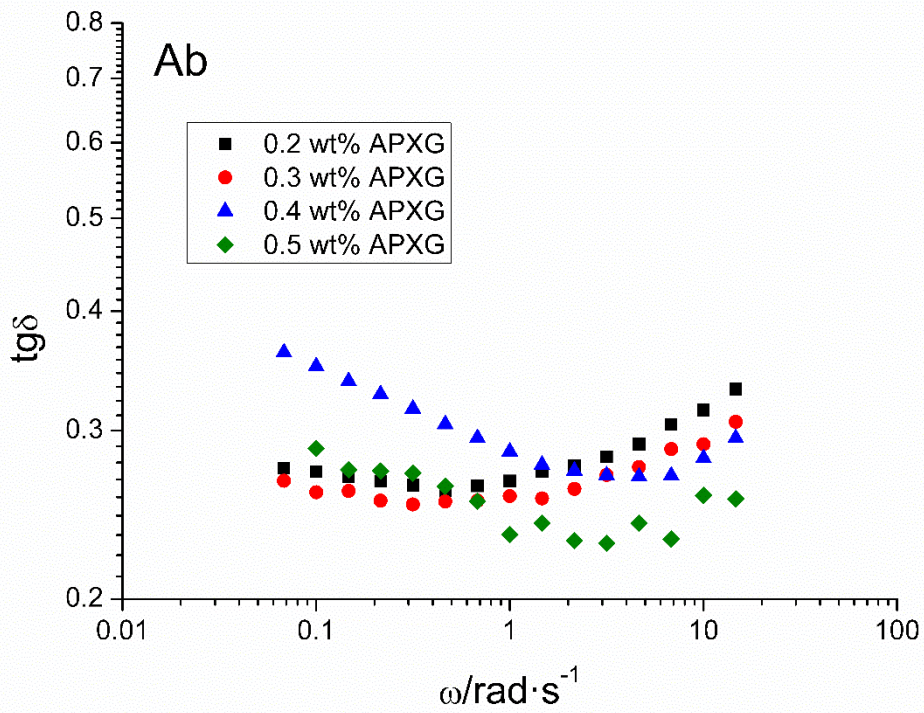


495

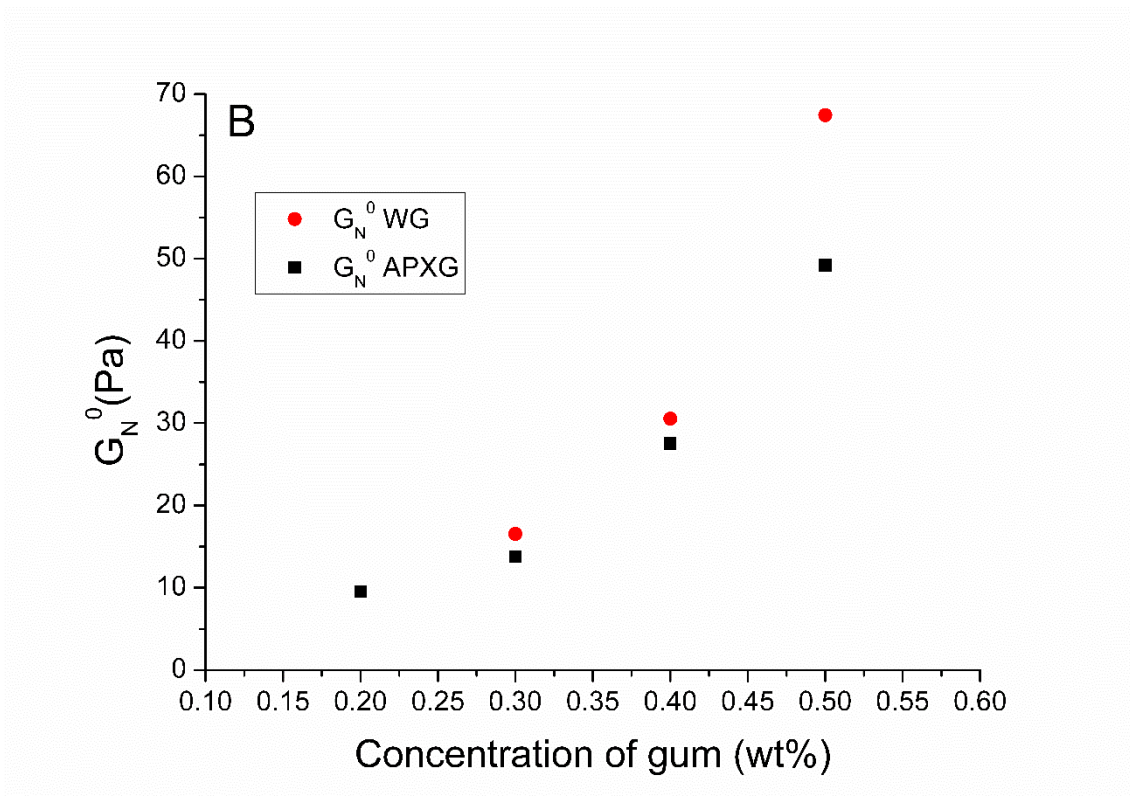
496 Figure 2. Influence of gum concentration on the mechanical spectra for nanoemulsions
 497 containing a) WG or b) APXG. Temperature = 20 °C.



498

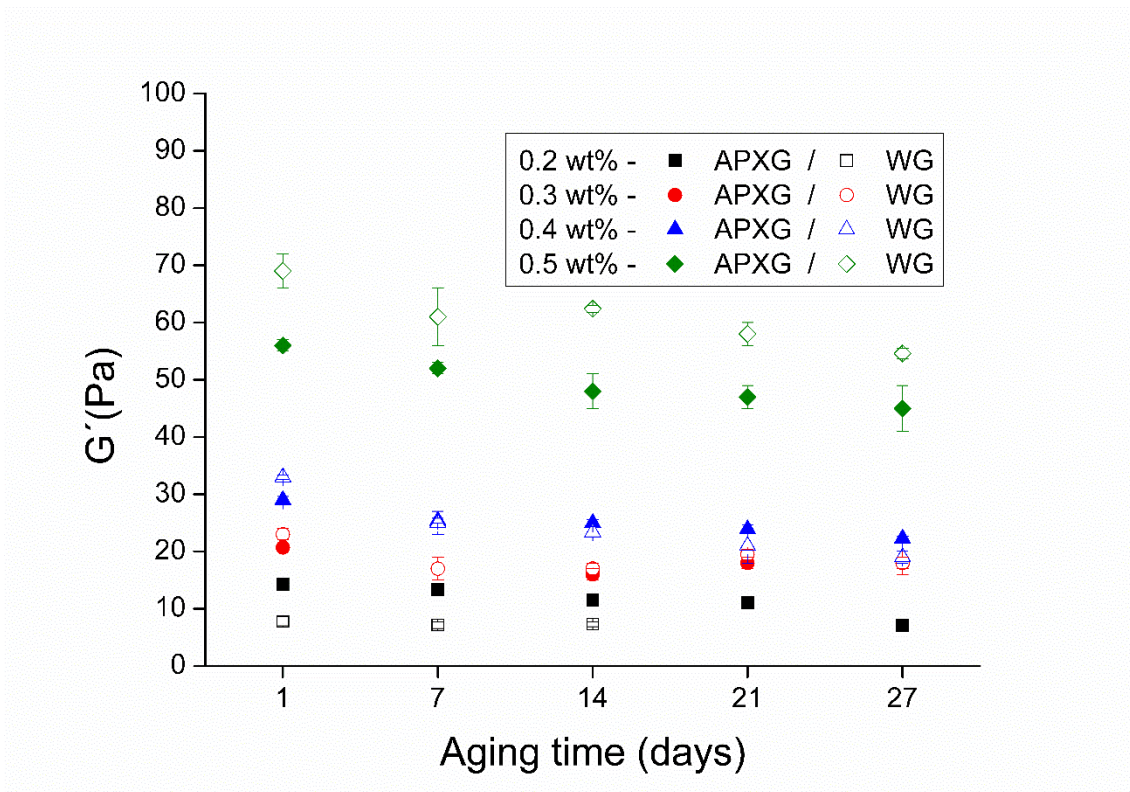


499



500

501 Figure 3. A) Influence of frequency on loss tangent of rosemary essential oil nanoemulsions 1-
 502 day aged containing a) WG or b) APXG as a function of the gum concentration. B) Plateau
 503 modulus of rosemary essential oil nanoemulsions versus gum concentration as a function of the
 504 type of gum.

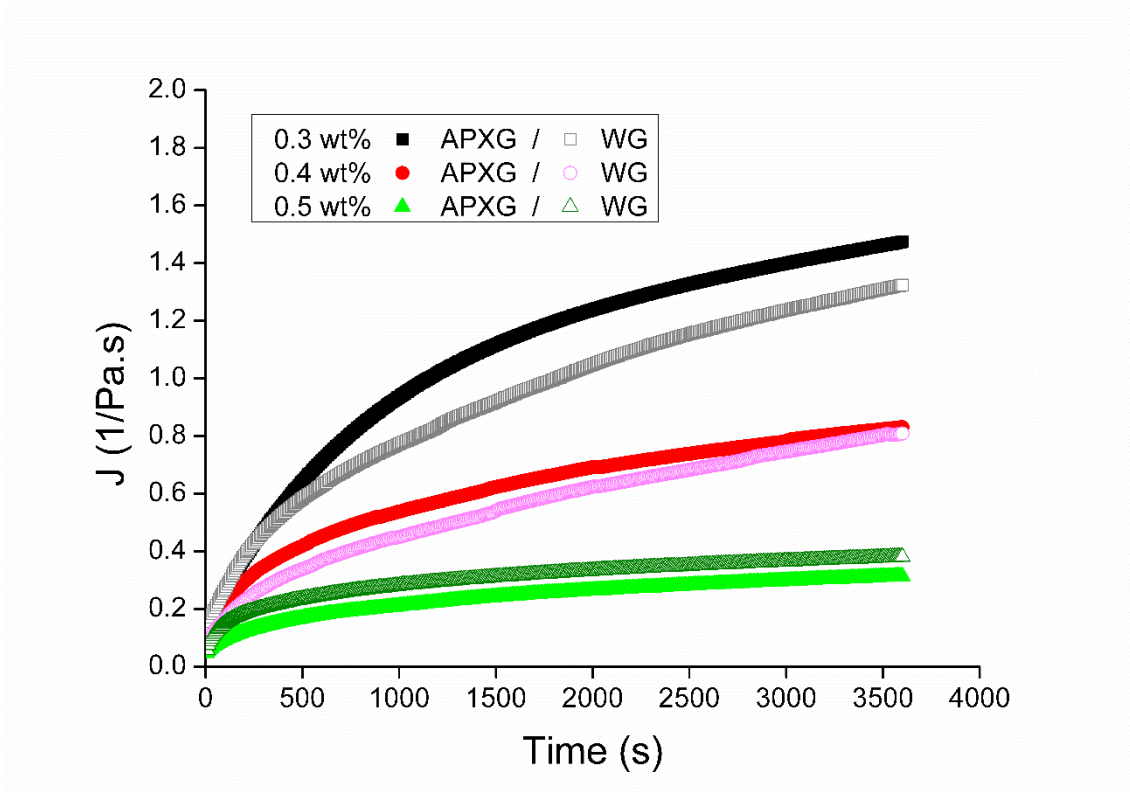


505

506

507 Figure 4. Influence of aging time on the elastic modulus at 6.8 rad/s of rosemary essential oil
508 nanoemulsions containing WG or APXG as a function of gum concentration. Temperature = 20
509 °C.

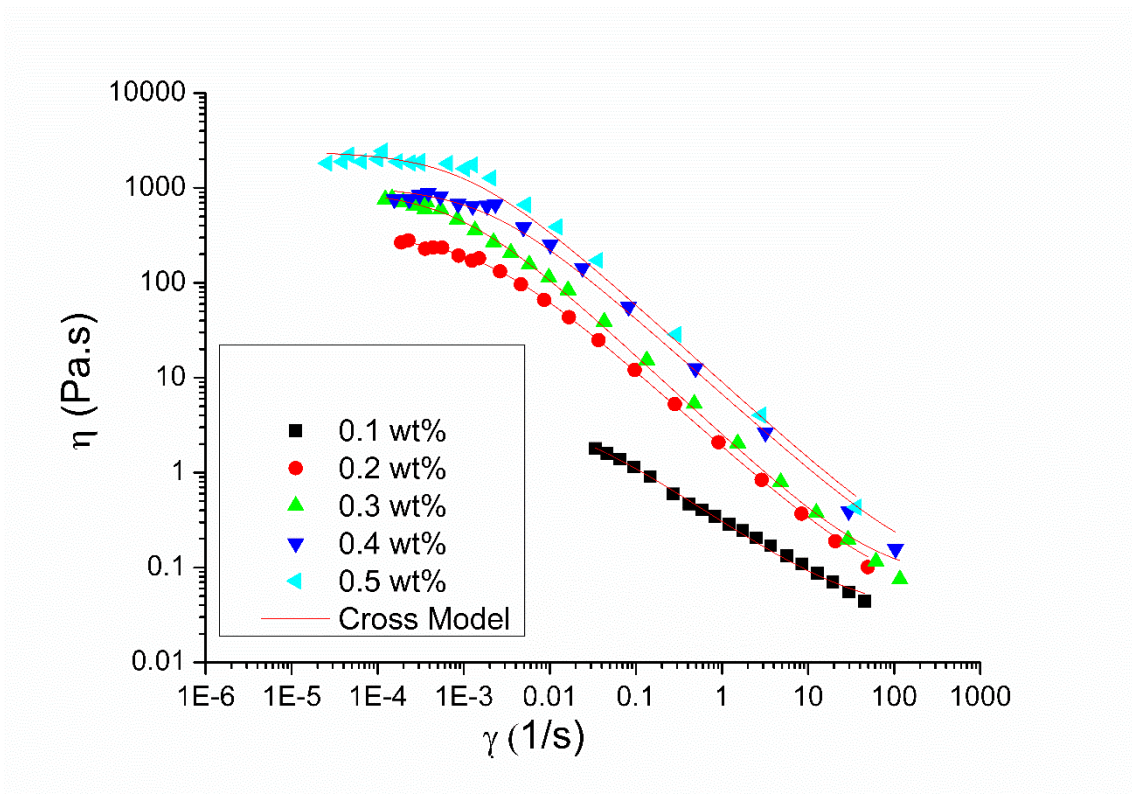
510



511

512 Figure 5. Creep compliance versus time of rosemary essential oil nanoemulsions containing WG
513 or APXG as a function of the gum concentration. Shear stress= 0.05 Pa. Temperature 20 °C.

514

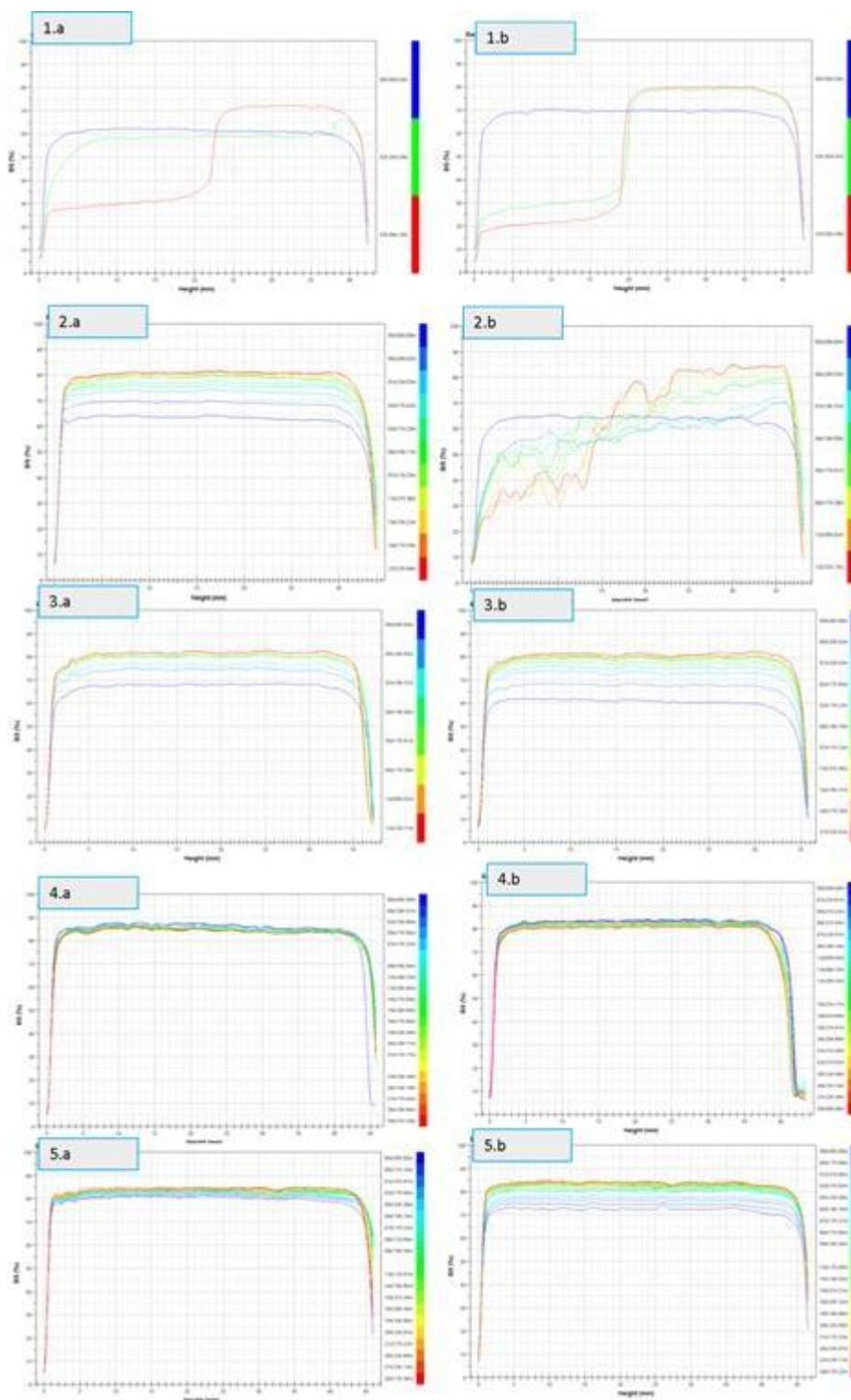


515

516

517 Figure 6. Flow curves of rosemary essential oil nanoemulsions containing different
 518 concentrations of APXG. Continuous lines correspond to the Cross model fitting equation.
 519 Temperature = 20 °C.

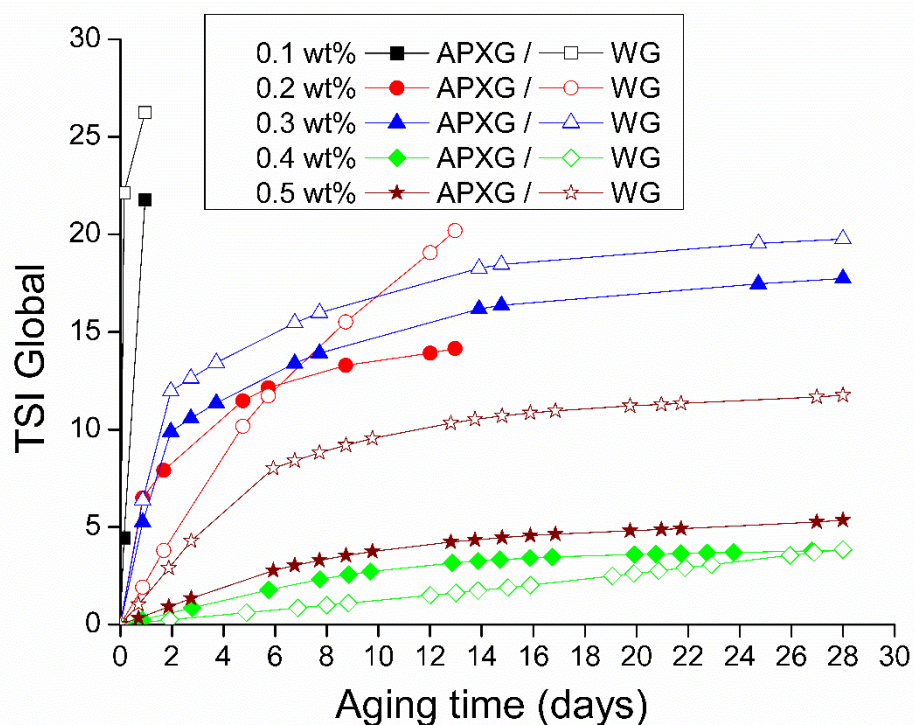
520



521

522 Figure 7. BS profiles versus measuring cell height of rosemary essential oil nanoemulsions
 523 containing a) APXG and b) WG at different concentrations of gum (1 (0.1/100g), 2 (0.2/100g),
 524 3 (0.3/100 g), 4 (0.4/100 g) and 5 (0.5/100 g) as a function of aging time.

525



526

527 Figure 8. Turbiscan stability index versus aging time of rosemary essential oil nanoemulsions
 528 containing WG (closed symbols) or APXG (open symbols) as a function of the gum concentration.
 529 Temperature = 20°C

530

531 **Tables**

532 Table 1. Volume mean diameter and span at 1 and 28 days of Rosemary essential oil
 533 nanoemulsions containing WG or APXG. Mean value \pm standard deviation values by a
 534 different superscripts within raw were significantly different ($P < 0.05$).

Gum concentration (wt%)	Gum	D _{4,3} - Day 1 (nm)	D _{4,3} - Day 28 (nm)	Span (Day 1)	Span (Day 28)
0.1	APXG	147 \pm 1 ^a	-	1.1 \pm 0.4 ^a	-
	WG	148 \pm 1 ^a	-	1.09 \pm 0.02 ^{a,b}	-
0.2	APXG	149 \pm 5 ^a	150 \pm 4 ^a	0.86 \pm 0.08 ^{a,b}	1.0 \pm 0.1 ^{a,b}
	WG	145 \pm 2 ^a	146 \pm 1 ^a	0.771 \pm 0.01 ^a	0.744 \pm 0.03 ^a
0.3	APXG	154 \pm 2 ^a	204 \pm 12 ^a	0.8 \pm 0.1 ^a	1.7 \pm 0.1 ^b

	WG	155±1 ^a	179±3 ^a	0.743±0.01 ^a	1.4±0.03 ^{a,b}
0.4	APXG	152±12 ^a	154±15 ^a	1.0±0.2 ^{a,b}	1.0±0.2 ^{a,b}
	WG	170±1 ^a	177±10 ^a	1.5±0.5 ^{a,b}	1.4±0.2 ^{a,b}
0.5	APXG	179±2 ^a	180±1 ^a	1.34±0.08 ^{a,b}	1.3±0.1 ^{a,b}
	WG	151±1 ^a	200±3 ^a	1.0±0.1 ^{a,b}	2.7±0.1 ^c

535

536

537 Table 2. Power law index of G' and G'' at 1 rad/s (b' , b'') and elastic and viscous
538 coefficient (a' , a''). Mean value ± standard deviation values by a different superscripts
539 within raw were significantly different ($P<0.05$).

Gum in nanoemulsion	a	SD _a	a'	SD _{a'}	b	SD _b	b'	SD _{b'}
WG	2.38 ^a	0.12	1.63 ^a	0.06	2.36 ^a	0.24	1.83 ^a	0.12
APXG	1.97 ^a	0.16	1.34 ^a	0.05	1.40 ^a	0.31	1.33 ^a	0.10

540

541 Table 3. Fitting parameters to the Burger model of creep tests results of rosemary
542 essential oil nanoemulsions 1 day aged containing WG or APXG. Mean value and
543 standard deviation values by a different superscripts within raw were significantly
544 different ($P<0.05$).

Concent. (wt%)	J_e^0 (1/Pa)		n_0 (Pa.s)		J_0 (1/Pa)		J_1 (1/Pa)		λ_1 (s)		J_2 (1/Pa)		λ_2 (s)	
	APXG	WG	APXG	WG	APXG	WG	APXG	WG	APXG	WG	APXG	WG	APXG	WG
0.2	1.3±0.5 ^a		7158±300 ^a		0.17±0.01 ^b		0.038±0.01 ^a		26.85±0.01 ^a		1.1±0.5		803.2±0.1 ^b	
0.3	0.8±0.5 ^a	0.75±0.07 ^a	9836±216 ^a	7625±1090 ^a	0.08±0.02 ^{a,b}	0.119±0.001 ^{a,b}	0.03±0.01 ^a	0.04±0.01 ^a	23.0±2 ^a	125±21 ^c	0.6±0.4	0.59±0.07	800±1 ^b	897±11 ^c
0.4	0.57±0.01 ^a	0.6±0.2 ^a	12698±1125 ^{a,b}	8235±1284 ^a	0.099±0.004 ^{a,b}	0.10±0.03 ^{a,b}	0.02±0.01 ^a	0.039±0.001 ^a	110±1 ^{b,c}	130±7 ^c	0.40±0.06	0.3±0.1	790±13 ^b	780±9 ^b
0.5	0.3±0.1 ^a	0.22±0.09 ^a	32840±5727 ^c	31997±6872 ^{b,c}	0.06±0.02 ^a	0.05±0.01 ^a	0.04±0.01 ^a	0.039±0.001 ^a	100±10 ^{b,c}	66±5 ^{a,b}	0.2±0.1	0.12±0.08	700±12 ^a	662±12 ^a

545

546 Table 4. Fitting parameters to the Cross model of flow curves of rosemary essential oil
547 nanoemulsions containing WG or APXG at 1 and 28 days of aging. Standar desviation: n_0
548 $< 10\%$. $n < 5\%$ and $\gamma_c < 10\%$. Mean value by a different superscripts within raw were
549 significantly different ($P<0.05$).

Concent. (wt%)	η_0 (Pa.s)		γ_c (s ⁻¹)		n	
	WG	APXG	WG	APXG	WG	APXG
0.1	3.36 ^a	4.93 ^a	0.031 ^b	0.014 ^a	0.43 ^h	0.33 ^g
0.2	67.73 ^a	316.45 ^{a,b}	1.6.10 ^{-3 a}	1.7. 10 ^{-3 a}	0.24 ^f	0.20 ^{e,f}
0.3	1000.50 ^{b,c,d}	934.31 ^{b,c,d}	6.6. 10 ^{-4 a}	1.0. 10 ^{-3 a}	0.18 ^{d,e}	0.16 ^{d,e}
0.4	1008.40 ^{b,c,d}	1042.73 ^{c,d}	4.8. 10 ^{-4 a}	2.0. 10 ^{-3 a}	0.14 ^{c,d}	0.10 ^{b,c}
0.5	3313.0 ^g	2414.74 ^f	4.0. 10 ^{-4 a}	1.1. 10 ^{-3 a}	0.13 ^g	0.07 ^{a,b}

550

551

Day 28	WG	APXG	WG	APXG	WG	APXG
0.2	164.14 ^a	90.59 ^a	1.3.10 ^{-3 a}	8.1. 10 ^{-3 a}	0.30 ^g	0.21 ^{e,f}
0.3	446.25 ^{a,b,c}	368.04 ^{a,b,c}	1.2. 10 ^{-3 a}	6.7. 10 ^{-3 a}	0.20 ^{e,f}	0.13 ^{c,d}
0.4	361.40 ^{a,b,c}	657.50 ^{a,b,c}	5.2. 10 ^{-3 d}	8.1. 10 ^{-3 a}	0.18 ^{d,e}	0.10 ^{b,c}
0.5	1924.4 ^{e,f}	1513.45 ^{d,e}	1.4. 10 ^{-3 c}	5.2. 10 ^{-3 a}	0.16 ^{d,e}	0.03 ^a